



Adaptive Overcurrent Protection for Microgrids in Extensive Distribution Systems

Lin, Hengwei; Guerrero, Josep M.; Jia, Chenxi; Tan, Zheng-Hua; Quintero, Juan Carlos Vasquez; Liu, Chengxi

Published in:

Proceedings of IECON 2016: The 42nd Annual Conference of IEEE Industrial Electronics Society

DOI (link to publication from Publisher):

[10.1109/IECON.2016.7793091](https://doi.org/10.1109/IECON.2016.7793091)

Publication date:

2016

Document Version

Early version, also known as pre-print

[Link to publication from Aalborg University](#)

Citation for published version (APA):

Lin, H., Guerrero, J. M., Jia, C., Tan, Z-H., Quintero, J. C. V., & Liu, C. (2016). Adaptive Overcurrent Protection for Microgrids in Extensive Distribution Systems. In *Proceedings of IECON 2016: The 42nd Annual Conference of IEEE Industrial Electronics Society* (pp. 4042 - 4047). IEEE Press.
<https://doi.org/10.1109/IECON.2016.7793091>

General rights

Copyright and moral rights for the publications made accessible in the public portal are retained by the authors and/or other copyright owners and it is a condition of accessing publications that users recognise and abide by the legal requirements associated with these rights.

- ? Users may download and print one copy of any publication from the public portal for the purpose of private study or research.
- ? You may not further distribute the material or use it for any profit-making activity or commercial gain
- ? You may freely distribute the URL identifying the publication in the public portal ?

Take down policy

If you believe that this document breaches copyright please contact us at vbn@aub.aau.dk providing details, and we will remove access to the work immediately and investigate your claim.

Adaptive Overcurrent Protection for Microgrids in Extensive Distribution Systems

Hengwei Lin¹ Josep M. Guerrero¹ Chenxi Jia²
hwe@et.aau.dk joz@et.aau.dk mobolo@163.com

1: Department of Energy Technology
Aalborg University,
9220 Aalborg East, Denmark

2: Department of Electrical Engineering
Beijing Jiaotong University,
Beijing, China

Zheng-hua Tan³ Juan C. Vasquez¹ Chengxi Liu⁴
zt@es.aau.dk juq@et.aau.dk chx@energinet.dk

3: Department of Electronic Systems
Aalborg University, 9220 Aalborg East, Denmark
www.microgrids.et.aau.dk

4: Energinet.dk
Tonne Kjærsvvej 65, Fredericia,
DK-7000, Denmark

Abstract—Microgrid is regarded as a new form to integrate the increasing penetration of distributed generation units (DGs) in the extensive distribution systems. This paper proposes an adaptive overcurrent protection strategy for a microgrid network. The protection coordination of the overcurrent relays is treated as a linear programming problem for the different operation states. In the control center, an artificial neural network (ANN) model is trained with real-time measurements to identify the states whether there is a fault on the line segment. Fault location is estimated further with the same measurements in another neural network model. Reconfigurations can be performed to modify the settings of the on-field relays to enhance the reliable operation for the different operational situations. The test results show that the adaptive overcurrent protection scheme with the assistance of estimation model can modify the protective settings for the new operation state accurately and intelligently.

Index Terms—artificial intelligence, adaptive overcurrent protection, distributed generation, distribution system, fault estimation, protection coordination, microgrid.

I. INTRODUCTION

Because of the concern of environment problems and the liberalization of the electricity market, high penetration of renewable energy sources (RES) have been integrated on the transmission and distribution systems. As the power system keeps developing toward to an intelligent entity, microgrid is hereafter considered as an effective way to accommodate numbers of DGs in the distribution system, which has special impact on the power flow, voltage regulation and network congestion etc. With flexible ancillary services provided for the consumers, microgrids can be operated in both grid-connected mode and intentional islanded mode [1], [2]. However, the increasing penetration of DGs also poses challenges to the protection of microgrids due to the bidirectional power flow, topology change and the intermittence of RES etc. Therefore, the protection should be enhanced to ensure the reliable and secure operation of the

entire system.

The fault current in one microgrid usually comprises the short-circuit current drawn from the connected main grids, DGs and rotating loads (such as the induction motors). In the situation, the short-circuit capability in some fault location may be higher than the withstanding short-circuit capability of the primary equipment. Meanwhile, DG connected with transformer and a single power electronics device have different contribution on the short-circuit current. To against the above problems, conventional protection with installation of fault current limiter (FCL) is proposed in [3]-[9]. In general, FCL is a series device which can be hidden in normal operation but can limit the instantaneous short-circuit current during a fault event [10]. The FCL can be installed on the feeder connecting the upstream and downstream network in a microgrid. For this installation of FCL, however, the limited current may decrease the power quality and the selectivity of protection in the downstream [11], especially when the topology and parameters change frequently in distribution system.

The conventional protection schemes in the distribution system are often designed for unidirectional power flow, but the high integration of DGs may lead to bidirectional power flow. The intermittence and randomness of RES may further bring variable infeed currents on the feeder so that the protection may lose the selectivity and sensitivity during a fault. Another applicable solution for microgrid is adaptive protection that can modify the protective settings response to a change in system conditions or requirements [12]. An adaptive distance protection scheme with transfer tripping function is proposed in [13] for a MV microgrid. An adaptive overcurrent scheme without communication is presented in [14]. In this reference, each relay records all the setting groups of all the other relays in the network so that the relay can identify the change of the topology operation mode to

modify the protective response. In [15], there is a main relay located at the substation controlling the downstream breakers dependent on real-time communication. In this case, the reliability of the protection scheme may be degraded once the main relay is out of order. In [16], another adaptive overcurrent protection scheme is proposed for microgrid with interlock function. The states of the network can be conformed and recorded as event tables in the control center.

In modern power system, the protection is often integrated with control and measurement as wide area measurement system (WAMS) and wide area control system (WACS) in transmission grids [17]. Based on the synchronized phasor measurement using a common clock from the global positioning system (GPS), some protection methods are proposed in [18]-[19]. Dependent on the modern supervisory control and data acquisition (SCADA) system, (adaptive) protection may play attractively for microgrids in extensive distribution systems to improve the observability, controllability and reliability of the entire system. As the industrial internet is regarded as the future tendency, the electricity supply utility is required to perform more intelligently and actively to support the future development. Therefore, this paper proposes an adaptive directional overcurrent protection with independent state estimation for the relays in microgrid which can be operated in a smart, automatic and reliable way.

The remainder of this paper is organized as follows: A medium voltage (MV) microgrid model is introduced in Section I. Section II describes the calculation of protective settings for different operation modes in the microgrid. In Section III, an adaptive protection scheme is proposed that can modify the setting groups with the assistance of the estimation model. Compared with the existing methods, the proposed scheme can perform in an intelligent and automatic way against the faults in the microgrid. The test result is given in Section IV, followed by the conclusion in Section V.

II. CONFIGURATION OF MICROGRID

The test microgrid is given in Fig.1, which contains a combined heat and power (CHP) plant and three small wind farms. There are three gas turbine generators in the CHP plant. Meanwhile, there are two 2WM doubly fed induction generators (DFIGs) and a 0.8MW capacitor bank in each small wind farm. The line impedance data is given in Table I. More details can be found in [13].

Normally, SCADA system in electric utilities has the ability to control the distribution-level equipment through distribution/substation automation system. However, the SCADA system usually is unable to control the smaller entities such as DGs, homes, and buildings. In one microgrid, there is often a data concentrator monitoring and controlling the on-field devices in the downstream network that can be regarded as an expanding intermediate level of the substation automation system. The configuration (primary and secondary

| line | Resistance (Ohm) | Reactance (Ohm) |
|--------|------------------|-----------------|
| Line12 | 1.24 | 1.21 |
| Line23 | 0.372 | 0.363 |
| Line34 | 0.992 | 0.968 |
| Line45 | 0.928 | 0.75 |
| Line56 | 0.2295 | 0.1875 |
| Line17 | 0.124 | 0.121 |
| Line16 | 1.224 | 1.0 |

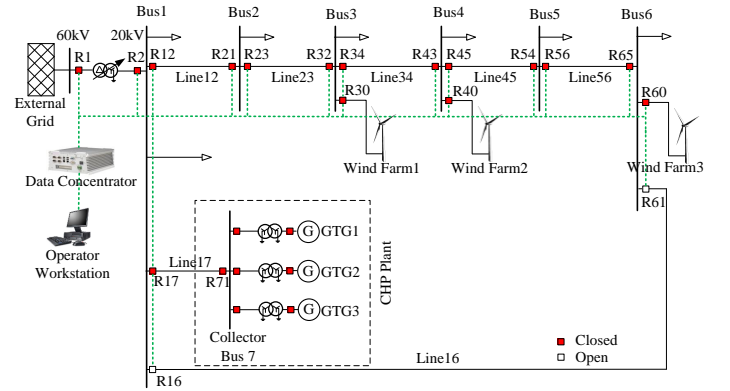


Fig. 1. The test microgrid model in Aalborg.

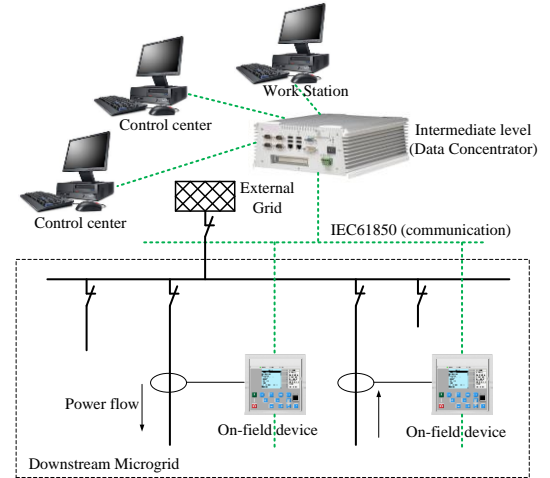


Fig. 2. The expanding substation/distribution automation system for microgrids in distribution system.

electric power equipment) of the expanding SCADA system in microgrid is given in Fig.2. The data concentrator transfers the data and information from the process to the higher level system and provides a central human machine interface (HMI) for the interaction between on-field devices, small entities and the utility operators. On the basis of the control model Generic Substation Events (GSE), simple network time protocol (SNTP) server or GPS controlled inter-range instrumentation group (IRIG) time code generator can be used for synchronizing the events. In this paper, the data concentrator and on-field relays have the synchronized phasor measurement capability to update the real-time clock. With the accuracy of less than 1us, the protective settings of the

relays can be modified accurately by the data concentrator.

III. PROTECTION COORDINATION

A. Protective Settings Coordination

Because the short-circuit current is significantly influenced by the operation modes and topologies, the protective settings require to be designed separately based on the current operational states of microgrid. There are four operational situations considered in the microgrid: grid-connected looped mode, grid-connected radial mode, islanded looped mode and islanded radial mode. The configuration can be modified by controlling the connection/disconnection of R2 and/or line16. Once a permanent fault or emergency occurs, reconfiguration can be performed automatically after the on-field actuator receives the command from data concentrator.

The adaptive protection scheme should first determine and implement the protective settings which are most appropriate for the coordination and the operation. The coordination algorithm is based on optimizing an objective function of operating times of the primary relays while subjected to maintaining the operation of backup relays coordinated. The objective function for a system contains m relays can be formulated as:

$$z = \text{Min} \sum_{f=1}^{f_{\max}} \left(\sum_i^m (t_{i,i} + \sum_j t_{i,j}) \right) \quad (1)$$

where: f indicates the fault location.

$t_{i,i}$ is the operating time for the primary relay located at i for a fault near at i .

$t_{i,j}$ is the operating time for the backup relay located at j for the same fault near at i .

The operating time $t_{i,j}$ for the backup relays should be larger than $t_{i,i}$, which can be expressed as below:

$$t_{i,j} \geq t_{i,i} + \Delta t \quad (2)$$

where Δt is the coordination time interval (CTI).

In this paper, the directional overcurrent relays (DORs) follow the IEC characteristic:

$$t = \frac{A \times TDS}{\left(\frac{I_f}{I_p} \right)^B - 1} \quad (3)$$

where: A is a constant

B is a characteristic index

I_f is the fault current magnitude

I_p is the pickup current

TDS is the time dial setting

I_p and TDS should be determined in a specific range as

given below:

$$TDS_{\min} \leq TDS \leq TDS_{\max} \quad (4)$$

$$I_{p,\min} \leq I_p \leq I_{p,\max} \quad (5)$$

Once the pickup current of relays are confirmed from the system requirements via power flow calculation and complete short-circuit analysis, the equation (3) can be written as:

$$t = a \times TDS \quad (6)$$

$$\text{where } a = \frac{A}{\left(\frac{I_f}{I_p} \right)^B - 1}$$

The objective function can be expressed as following:

$$z = \text{Min}(\lambda_1 \times TDS_1 + \lambda_2 \times TDS_2 + \dots + \lambda_m \times TDS_m) \quad (7)$$

Equation (2) can be rewritten as the form of (7):

$$a_{i,j} \times TDS_j \geq a_{i,i} \times TDS_i + \Delta t \quad (8)$$

Equation (7) and (8) form a linear optimization problem which can be solved by linear programming.

B. Short-circuit Calculation

In this paper, the fault calculation is based on IEC 60909. The total fault current is the vector sum of all the devices such as external grid, DGs, transformer and loads etc. In the case of three-phase fault, the initial short-circuit can be calculated by:

$$I_k'' = \frac{c U_n / \sqrt{3}}{Z_k} \quad (9)$$

where U_n is the phase to phase voltage of the system sources. c is the voltage factor that equals to 1.1 in the calculation. Z_k is the impedance through which the short-circuit current flow from the generator to the fault location of the fault. This is indeed the positive-sequence impedance per phase:

$$Z_k = \sqrt{(\sum R)^2 + (\sum X)^2} \quad (10)$$

where $\sum R$ is the sum of series resistances while $\sum X$ is the sum of series reactances.

The impedance may be calculated after separately summing the various resistances and reactances from the power sources to the fault location in the fault network. The impedance of distribution transformer Z_{TK} can be calculated:

$$Z_{TK} = K_T Z_T \quad (11)$$

$$K_T = 0.95 \frac{C_{\max}}{1 + 0.6 x_T} \quad (12)$$

where C_{\max} is the voltage factor related to the normal voltage at the low-voltage side of the network transformer. x_T is the relative reactance of the transformer:

$$x_T = X_T \frac{S_{rT}}{U_{rT}^2} \quad (13)$$

Table II. Forward fault current and load current

| Forward direction | Maximum fault current I_{fmax} (kA) | Minimum fault current I_{fmin} (kA) | Anticipated Maximum load current I_{kmax} (kA) | Time dial setting (TDS) |
|-------------------|---------------------------------------|---------------------------------------|--|---------------------------------|
| Line12 | 8.15/6.84/ 3.34/2.02 | 1.79/1.48/ 1.31/0.73 | 0.22/0.3/ 0.2/0.24 | 0.0936/0.0576/ 0.0996/0.0708 |
| Line23 | 3.35/3.54/ 1.78/1.58 | 0.99/0.97/ 0.72/0.53 | 0.21/0.27/ 0.18/0.22 | 0.0808/0.0523/ 0.0895/0.0609 |
| Line34 | 3.63/3.93/ 2.37/2.34 | 1.14/1.21/ 0.98/0.93 | 0.18/0.23/ 0.16/0.2 | 0.0728/0.0463/ 0.077/0.0488 |
| Line45 | 3.54/4.04/ 2.80/3.26 | 1.08/1.52/ 1.09/1.38 | 0.16/0.20/ 0.15/0.15 | 0.0588/0.035/ 0.0589/0.039 |
| Line56 | 2.34/2.95/ 1.87/2.57 | 0.64/1.25/ 0.67/1.14 | 0.15/0.17/ 0.13/0.12 | 0.0399/0.02/ 0.0409/0.02 |
| Line16 | 7.92/-/ 3.09/- | 1.71/-/ 1.19/- | 0.13/-/ 0.1/- | 0.02/-/ 0.02/- |

Table III. Backward fault current and load current

| Backward direction | Maximum fault current I_{fmax} (kA) | Minimum fault current I_{fmin} (kA) | Anticipated Maximum load current I_{kmax} (kA) | Time dial setting (TDS) |
|--------------------|---------------------------------------|---------------------------------------|--|---------------------------------|
| Line12 | 1.16/1.90/ 1.19/1.96 | 0.15/0.21/ 0.35/0.58 | 0.15/0.1/ 0.16/0.08 | 0.02/0.02/ 0.02/0.02 |
| Line23 | 2.65/2.48/ 2.26/2.55 | 0.77/0.59/ 0.87/0.85 | 0.16/0.13/ 0.18/0.12 | 0.0398/0.0409/ 0.0373/0.041/ |
| Line34 | 2.31/1.82/ 1.79/1.88 | 0.70/0.45/ 0.70/0.60 | 0.17/0.15/ 0.19/0.14 | 0.0579/0.0589/ 0.0539/0.0599 |
| Line45 | 2.47/0.84/ 1.53/0.86 | 0.75/0.22/ 0.60/0.26 | 0.2/0.17/ 0.23/0.15 | 0.0683/0.0737/ 0.610/0.0789 |
| Line56 | 3.85/0.89/ 2.36/0.91 | 1.16/0.34/ 0.99/0.37 | 0.22/0.18/ 0.24/0.16 | 0.0789/0.0895/ 0.0732/0.961 |
| Line16 | 1.41/-/ 1.44/- | 0.20/-/ 0.44/- | 0.24/-/ 0.26/- | 0.0874/-/ 0.0810/- |

The ratio R_G/X_d'' for DGs can be considered as 0.15 [11], so that the impedance of the DGs can be calculated by:

$$R_G = \left(\frac{R_G}{X_d''} \right) x_d'' \left(\frac{U_{rG}^2}{S_{rG}} \right) \quad (14)$$

$$Z_G = K_G (R_G + X_G) \quad (15)$$

where K_G is the correction factor during the calculation.

Through using the above equations, the short-circuit currents are calculated for the test network with the relevant parameters in Digsilent PowerFactory. The short-circuit current and power flow both for forward and backward directions are given in Table II and Table III based on different fault location, fault impedance and load conditions. The results contain all the four operation modes in sequence: gird-connected looped mode, gird-connected radial mode, islanded looped mode, and islanded radial mode which are distinguished with backslashes. It can be found that the fault current changes severely for forward direction relays among the different operation modes. For the backward direction relays in Table III, however, the fault currents (I_{fmax} and I_{fmin}) in the two radial operation modes have almost the same results. Moreover, the load flow currents (I_{kmax}) are relatively

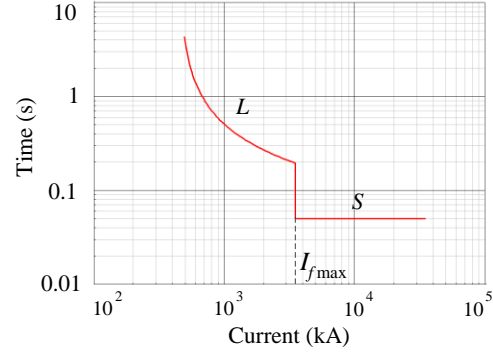


Fig. 3. The characteristic curve of DOR

small due to the existence of high penetration of DGs near the load consumption.

In this paper, the instantaneous tripping part of a directional overcurrent relay is inactivated for simplification purpose. As is shown in Fig.3, the tripping curve consists of a constant time delay part S (protection against short-circuit with certain time delay) and the above mentioned inverse time part L (protection against overload and short-circuit). In order to provide a selective operation for different relays, the maximum fault currents I_{fmax} are used to separate/connect the two tripping parts.

The relay settings for adaptive protection are mainly based on the selected operating conditions. The pickup settings of phase fault overcurrent protection should be determined considering both the fault and load currents. With the decrease of the load currents, the pickup settings are reduced but should be kept more than the maximum anticipated load current in the next several hours. To avoid the unnecessary tripping and to keep the selectivity, the coordination time interval CTI is selected as 0.1s and the pickup current I_p is 1.5 times of the maximum load current I_{kmax} . After selecting the fault currents and the pickup current, the optimized time among the relays can be obtained. In practical application, the protective settings may need some additional check and adjustment for the reliability requirements. The final adopted TDS in this paper are given in Table II and III. It can be found that the TDSs for grid-connected mode and islanded mode are different due to the different operation parameters.

IV. ADAPTIVE PROTECTION SCHEME

After the calculation of optimal protective setting groups, the relay settings are separately sent to and recorded in the corresponding on-field relays through the remote control form the utility control center. Meanwhile, the relay settings should be modified in time once the operation states are changed in the downstream network. As is mentioned in section II, with the collected measurements from the on-field devices, the data concentrator can assist the system operators on state estimation and decision making tasks in an automatic way. The flow diagram of the proposed adaptive overcurrent protection scheme is given in Fig.4. Once a fault happens, the tripping action activates the on-field measurements retrieval,

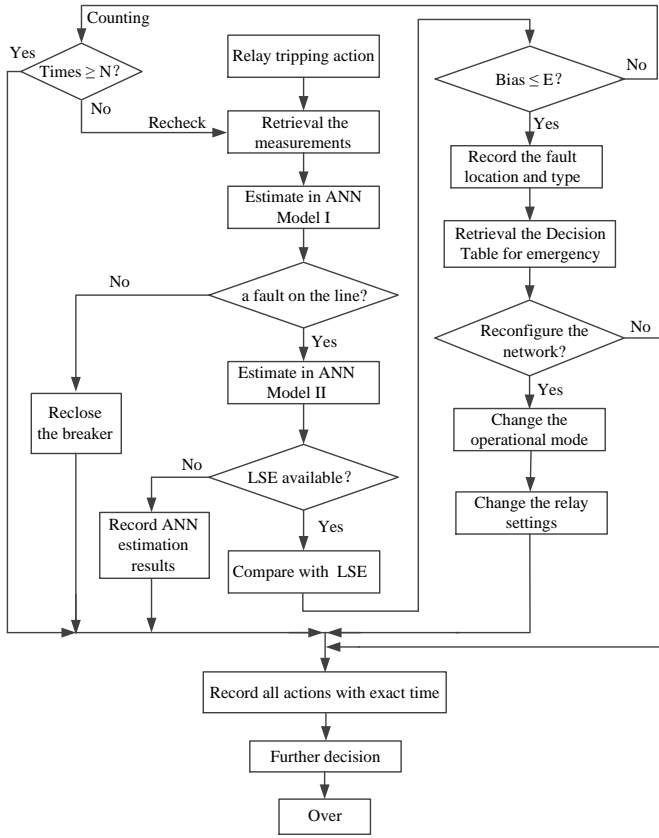


Fig. 4. Flow chat of the adaptive overcurrent protection scheme.

and sends them to estimation Model I to identify whether there is a fault. If it is confirmed that a fault occurs on the feeder, fault location estimation is performed in Model II. Otherwise, the breaker is reclosed after certain delay. The estimated fault location can be compared with the least square estimation (LSE) results collecting from the on-field devices for redundancy requirements. If the bias between the two estimation results is less than a value E (or LSE is unavailable), the result is recorded with the average estimated value. Otherwise, the estimation is rechecked based on the real-time measurements. Then, an advanced decision table is retrieved to decide whether to reconfigure the network and the protective settings. Finally, the decision is confirmed and sent to the actuator to perform. All the actions are recorded with exact time for further analysis.

Artificial neural network is a non-linear machine learning model. An ANN contains a lot of elementary neurons which are connected together in various architectures that are inspired by biological neural networks. In ANN models, the feed-forward neural network that is also known as the multilayer perceptron (MLP) is most popular. As is shown in Fig.5, there are numbers of neurons in each layer of MLP taking inputs from the previous layer neurons. There are some excitation signals feeding into the input layer. The neuron is a nonlinear model acting as a logistic regression of its inputs. As is shown in Fig.6, every neuron generates an output as a weighted (w) input for the next layer. Meanwhile,

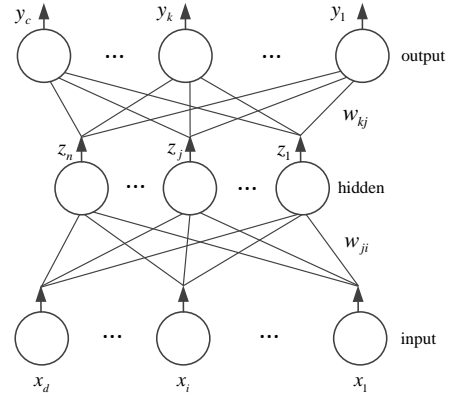


Fig. 5. The illustration of ANN.

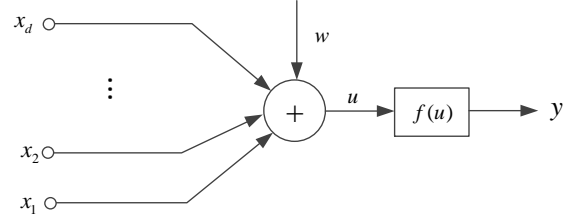


Fig. 6. The illustration of a single neuron model.

TABLE IV. The Error of ANN Model I

| Layers | error for test cases | error for all cases |
|--------|----------------------|---------------------|
| 2 | 0 | 0 |
| 3 | 0 | 0 |
| 4 | 0 | 0 |
| 5 | 0 | 0 |

TABLE V. The Error of ANN Model II

| Layers | Average error for test cases (%) | Average error for all cases (%) |
|--------|----------------------------------|---------------------------------|
| 2 | 0.63 | 0.21 |
| 3 | 0.52 | 0.13 |
| 4 | 0.51 | 0.21 |
| 5 | 0.8 | 0.25 |

the neurons are connected through links between different layer. During the training process, the weight and the bias of each neuron are adjusted according to the training data. Then, the ANN can be used for testing or actual applications. ANN is often considered as a typical representative of artificial intelligent. The ANN models are determined by the network architecture, transfer function and learning rules. One of central tasks during designing ANNs is to find the appropriate architecture and weights for the network. In general, ANNs are designed by means of trial and error and fixed during the learning process and the parameters are trained by gradient-based algorithms liable to converge to a local minimum.

The training and test for ANNs are implemented in MATLAB. The 'logistic' transfer function is adopted for signal delivering between the neurons of two layers. For adjusting the weights and biases in ANNs, back propagation learning rule is performed to obtain minimized quadratic sum error of ANN network. In this paper, 65% of the available data are selected randomly as the training set while the remaining data are adopted for test.



Fig. 7. The error of ANN Model II.

ANN model I is designed and trained to reveal whether there is a fault on this feeder. The accuracy of ANN model I is always 100% as is observed in Table IV. The result is reasonable because the model uses two-terminal phasors measurement working as the input signals in the estimation model which contains the directional information for each feeder. Meanwhile, the test results for different numbers of hidden neurons of ANN Model II are given in Table V and Fig.7. The errors in all the tests are less than 1%, which are acceptable for state estimation.

V. CONCLUSION

According to the analysis, the optimization of protection coordination can be solved as a linear programming problem. An adaptive overcurrent protection scheme based on the synchronous phase measurement is proposed for different operation modes in microgrid. For the upcoming intelligent industrial energy internet, two ANN models are integrated in the distribution automation system to assist the operators making decisions and to provide accurate estimated information. With the deployment of the modern communication and measurement system in microgrids, the protection scheme can modify the protective settings intelligently and automatically in the extensive distribution systems.

REFERENCES

- [1] R. H. Lasseter, "MicroGrids," in *Power Engineering Society Winter Meeting*, vol.1, 2002.
- [2] L. Hengwei, L. Chengxi, J. M. Guerrero, J. C. Vasquez, and T. Dragicevic, "Modular power architectures for microgrid clusters," in *Green Energy*, pp. 199-206, 2014.
- [3] R. M. C. Abyaneh, H. A. Agheli, and A. H. Rastegar, "Overcurrent relays coordination considering transient behavior of fault current limiter and distributed generation in distribution power network," *Proc. Inst. Elect. Eng., Gen., Transm., Distrib.*, vol. 5, no. 9, pp. 903-911, 2011.
- [4] A. Conde and E. Vazquez, "Application of a proposed overcurrent relay in radial distribution networks," *Elect. Power Syst. Res.*, vol. 81, pp.570-579, 2011.
- [5] W. J. Park, B. C. Sung, K. B. Sung, and J. W. Park, "Parameter optimization of SFCL with wind-turbine generation system based on its protective coordination," *IEEE Trans. Appl. Supercond.*, vol. 21, no. 3, pp. 2153-2156, 2011.
- [6] W. J. Park, B. C. Sung, and J.W. Park, "The effect of SFCL on electric power grid with wind-turbine generation system," *IEEE Trans. Appl. Supercond.*, vol. 20, no. 3, pp. 1177-1181, 2010.
- [7] E. A. Swissi, R. M. Tumilty, N. K. Singh, G. M. Burt, and J. R. McDonald, "Analysis of transient stability enhancement of LV-connected induction microgenerators by using resistive-type fault current limiters," *IEEE Trans. Power Syst.*, vol. 25, no. 2, pp. 885-893, May 2010.
- [8] J. F. Moon, S. H. Lim, J. C. Kim, and S. Y. Yun, "Assessment of the impact of SFCL on voltage sags in power distribution system," *IEEE Trans. Appl. Supercond.*, vol. 21, no. 3, pp. 2161-2164, 2011.
- [9] W. El-Khattam and T. S. Sidhu, "Restoration of directional overcurrent relay coordination in distributed generation systems utilizing fault current limiter," *IEEE Trans. Power Del.*, vol. 23, no. 2, pp. 576-585, Apr. 2008.
- [10] P. G. Slade, J.-L. Wu, E. J. Stacey, W. F. Stubler, R. E. Voshall, J. J. Bonk, J. W. Porter, and L. Hong, "The utility requirements for a distribution fault current limiter," *IEEE Trans. Power Del.*, vol. 7, no. 2, pt. 1, pp. 507-515, Apr. 1992.
- [11] Ghanbari T, Farjah E. "Unidirectional fault current limiter: an efficient interface between the microgrid and main network," *IEEE Trans. Power Systems*, pp. 1591-1598., 2013
- [12] G. D. Rockefeller, C. L. Wagner, J. R. Linders, K. L. Hicks, and D. T. Rzy, "Adaptive transmission relaying concepts for improved performance," *IEEE Trans. Power Delivery*, vol. 3, pp. 1446-1458, 1988.
- [13] L. Hengwei, J. M. Guerrero, J. C. Vasquez, L. Chengxi, "Adaptive Distance Protection for Microgrids" in *IECON, Japan, Yokohama*, Nov. 2015.
- [14] P. Mahat, C. Zhe, B. Bak-Jensen, and C. L. Bak, "A Simple Adaptive Overcurrent Protection of Distribution Systems With Distributed Generation," *IEEE Trans. Smart Grid*, vol. 2, pp. 428-437, 2011.
- [15] S. M. Brahma and A. A. Girgis, "Development of adaptive protection scheme for distribution systems with high penetration of distributed generation," *IEEE Trans. Power Delivery*, vol. 19, pp. 56-63, 2004.
- [16] A. Oudalov and A. Fidigatti "Adaptive network protection in microgrids," *International J. Distributed Energy Resources*, pp. 201-226, 2009.
- [17] J. De La Ree, V. Centeno, J. S. Thorp, and A. G. Phadke, "Synchronized Phasor Measurement Applications in Power Systems," *IEEE Trans. Smart Grid*, vol. 1, pp. 20-27, 2010.
- [18] J. Joe-Air, Y. Jun-Zhe, L. Ying-Hong, L. Chih-Wen, and M. Jih-Chen, "An adaptive PMU based fault detection/location technique for transmission lines. I. Theory and algorithms," *IEEE Trans. Power Delivery*, vol. 15, pp. 486-493, 2000.
- [19] J. Joe-Air, L. Ying-Hong, Y. Jun-Zhe, T. Tong-Ming, and L. Chih-Wen, "An adaptive PMU based fault detection/location technique for transmission lines. II. PMU implementation and performance evaluation," *IEEE Trans. Power Del.*, vol. 15, pp. 1136-1146, 2000.